Int J Earth Sci (Geol Rundsch) (2016) 105:1471–1483
DOI 10.1007/s00531-015-1265-0

ORIGINAL PAPER

Formation and preservation of biotite-rich microdomains in high-temperature rocks from the Antananarivo Block, Madagascar

Bénédicte Cenki-Tok[1] · Alfons Berger[2] · Frédéric Gueydan[1]

Received: 5 May 2015 / Accepted: 9 October 2015 / Published online: 28 October 2015

Abstract Highly restitic rocks from the Antananarivo Block in northern Madagascar are investigated in this study in order to unravel processes of H_2O-rich biotite formation in HT rocks. Polyphase metamorphism and melt migration occurred at 0.6 GPa and 850 °C. Biotite remains stable together with orthopyroxene and makes up to 45 vol% of the rock. In addition, three well-characterised and delimited microdomains having different textural, chemical and petrological characteristics are preserved. Thermodynamic models using the specific bulk compositions of the domains are in agreement with petrological observations. These rocks provide evidence that the lower crust may be strongly heterogeneous, locally associated to the formation of hydrous restites controlled by episodes of melt production and melt escape. This has significant consequences for understanding of the lower crust.

Keywords Madagascar · High-temperature metamorphism · Granulites · Biotite · Microdomain · Lower crust

Introduction

In the past decade high-temperature (HT) granulites have been described all around the world (e.g. Vielzeuf et al. 1990; Harley 1998a; Brown 2002; Kelsey and Hand 2014). Such rocks are intensively investigated because they preserve assemblages reflecting extreme *P–T* conditions and show spectacular textures helping to decipher processes related to partial melting in the deep crust (Rickers et al. 2001; McFarlane et al. 2003; Harley 2008; Kelsey 2008). Calibrated petrogenetic grids combined with geothermometry helped to infer complex *P–T* paths in numerous localities for these rocks of extraordinary composition (Harley et al. 1990; Raith and Harley 1998; Carrington and Harley 1995; Harley 1998b; McDade and Harley 2001; Rickers et al. 2001; Goncalves et al. 2004; Sajeev and Osanai 2004; Baldwin et al. 2005; Kelsey et al. 2005; White et al. 2001, 2004, 2007; Diener et al. 2008).

The occurrence of local microdomains is commonly reported in rocks at amphibolite and eclogite facies conditions (e.g. Tòth et al. 2000; Brouwer and Engi 2005). By contrast, HT rocks can be divided into migmatites (which are rocks including different domains per definition) and granulites, which are often homogeneous and equilibrated (Thompson 1990). It is generally considered that granulites form under relatively dry metamorphic conditions (e.g. Buddinton 1952; Turner 1981). These may be the result of removal of water by dissolution in (escaped) melts (Powell 1983; McKenzie and Jackson 2002) or the presence of CO_2 (possibly mantle-derived) that changes the H_2O activity. The presence/absence of water or melt in the lower crust is a major controlling parameter for the continental lithosphere rheology (Jackson 2002), and hence, it is important to constrain from field observation its possible mineralogical heterogeneity.

In this study, we report the occurrence of microdomains in HT rocks from Madagascar. These rocks contain up to 44 vol% of biotite. The aim of this study is to: (a) report that textural heterogeneities as well as H_2O-rich biotite are present in these HT rocks with a detailed petrographic work

✉ Bénédicte Cenki-Tok
cenkitok@gm.univ-montp2.fr

[1] UMR-CNRS 5243 Géosciences Montpellier, Université Montpellier, Place E. Bataillon, 34000 Montpellier, France

[2] Institut für Geologie, Baltzerstrasse 1+3, 3012 Bern, Switzerland

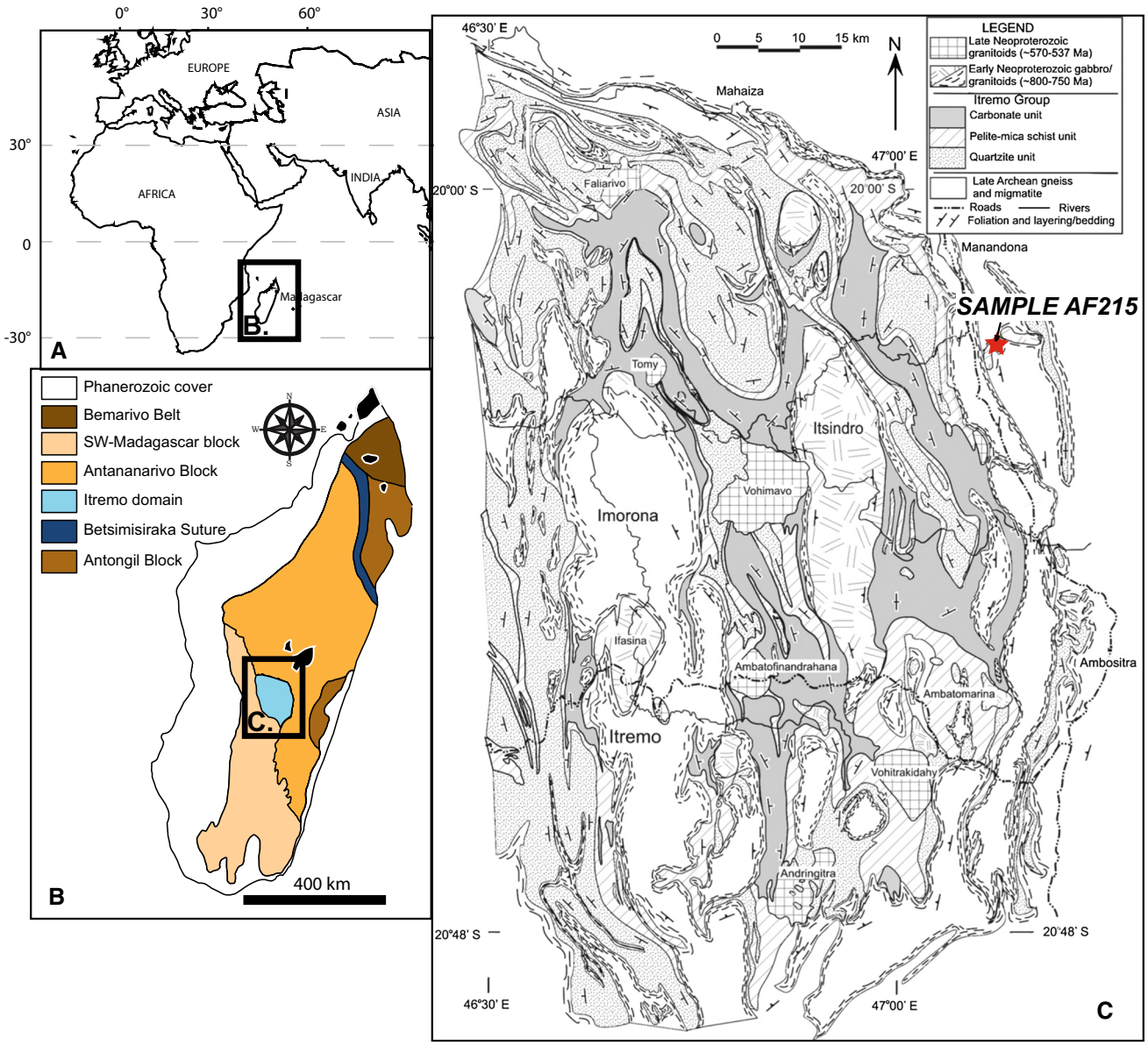

Fig. 1 **a** *Inset* showing the location of Madagascar compared to Africa and Eurasia. **b** Simplified map of Madagascar presenting the major units. **c** Petro-structural map showing the area in which the studied sample AF215 is located (modified after Tucker et al. 2007)

(b) explain the mode of formation and preservation of these microdomains by elaborating thermodynamic models and calculating *P–T* estimates, and (c) discuss possible implications for our understanding of the lower crust.

Geological setting

The Antananarivo block is a major basement unit in central Madagascar (Fig. 1a, b). This terrane underwent a major metamorphic event during East African Orogenesis at Neoproterozoic to Cambrian time (Martelat et al. 1999, 2000; Berger et al. 2006; Giese et al. 2011; Tucker et al. 2014 and references therein). It mainly consists of prominent, predominantly north–south trending migmatites, granites, micaschists and gneisses (Windley et al. 1994) metamorphosed under granulite to upper-amphibolite facies (Collins 2006). The block is characterised by late Archean granitoids (~2.5 Ga; the Betsiboka Suite) tectonically interlayered with paragneisses of the Ambatolampy Group (Archibald et al. 2015) that are intruded by granites, syenites and gabbros dated at ~760–820 Ma (Handke et al. 1999; Tucker et al. 1999; Kröner et al. 2000). The Itremo Group belongs to a series of Proterozoic metasedimentary units structurally overlying the Antananarivo Block (Cox et al. 2004). During Pan-African orogeny (between 550 and

Table 1 Results of EMPA monazite age dating

Th (ppm)	U (ppm)	Pb (ppm)	Age (Ma)	Error (2 sigma)
67,400	1069	2564	798.4	14.4
68,200	2083	2709	796.7	13.0
64,200	999	2399	785.4	14.5
25,100	1138	940	720.8	26.3
53,300	2196	2196	826.2	16.1
28,300	1492	1221	810.4	28.2
	Weighted mean		795.6	27.4

490 Ma), the Antananarivo block as a whole was affected by amphibolite to granulite facies metamorphism (Kröner et al. 2000) as well as associated magmatism (Tucker et al. 1999; Handke et al. 1999; McMillan et al. 2003; Tucker et al. 2014). Locally, the adjacent Andriamena unit and Bemarivo Belt (Fig. 1b) contain indications for a distinct HT granulite facies metamorphism at roughly 800 Ma (Goncalves et al. 2004; Jöns et al. 2006), but relics of this older event are rare in the Antananarivo block. The sample studied (AF215; 47°07′38.3E/20°10′29.3S; Fig. 1c) is one of these relics. It was collected from the Antananarivo block and belongs to an enclave within an early Neoproterozoic granitoid. Monazite grains in this sample preserve Neoproterozoic ages (ca. 796 Ma, Table 1) and are not overprinted by the Pan-African metamorphic event.

Methods

Mineral compositions were determined with a JEOL JXA 8200 electron probe at the University of Bern, operating at 15-kV accelerating voltage and 15-nA beam current. Data processing was performed with the ϕ–ρ–z correction procedure. For monazite age dating, complete analysis was done using an elemental line set-up similar as described in Scherrer et al. (2000). We used 25-kV acceleration voltage, 50-nA beam current as well as silicate and phosphate standards. Conventional geothermobarometers were applied using the programme GTB (Kohn and Spear 2001). Aluminium in orthopyroxene thermometry was performed using the calibration of Harley and Green (1982) and Aranovich and Berman (1997). In order to determine the bulk chemical composition of the different domains, the modal abundance of each mineral phase was estimated by BSE image analysis with ImageJ software. Representative microprobe analyses (in wt%) were integrated over the calculated area for each mineral and summed to yield the bulk composition (in wt%) of the domains of interest. Given the small grain size (<1 mm, even <500 µm for domain A) compared to thin section area (ca. 1276 mm^2) and the homogeneity of equilibrated textures and mineral chemistry, we consider that the surface estimation of modal abundance of minerals is representative of the volume modal abundance of minerals. For thermodynamic calculations in the simplified model system Na_2O–CaO–K_2O–FeO–MgO–Al_2O_3–SiO_2–H_2O–TiO_2, the database of Holland and Powell (1998) (thermodynamic database of THERMOCALC, version 3.21) was used including recent updates (Holland and Powell 1998; Baldwin et al. 2005; Kelsey et al. 2005; White et al. 2007). Solution models for feldspars is taken from Baldwin et al. (2005); ilmenite, garnet, biotite, spinel and liquid is from White et al. (2007); orthopyroxene is from White et al. (2002); amphibole is from Diener et al. (2007); and cordierite is from Holland et Powell (1998). Rock-specific equilibrium assemblage diagrams were calculated with the free energy minimisation programs THERIAK and DOMINO (de Capitani and Brown 1987; de Capitani and Petrakakis 2010). More detail about the software is available: http://titan.minpet.unibas.ch/minpet/theriak/theruser.html. Mineral abbreviations used are from Whitney and Evans (2010).

Results

Petrography

Sample AF215 is a fine-grained dark-coloured rock. The hand specimen presents a patchy texture composed of three different domains (Fig. 2a). Domain A shows mm-sized plagioclase in a dark matrix composed of orthopyroxene and biotite. Domain B is richer in biotite and orthopyroxene and contains rare plagioclase. Domain C consists in a layer of pink cm-sized garnets crystals with rare inclusions of orthopyroxene and biotite. Contacts between the domains are anastomosing. There is no gneissic layering. The observed mineral assemblages are highly restitic (Table 2), evidence of crystallized melt is rare (see below), but its presence is most likely given the geological and petrological setting.

In thin section, the three microdomains of sample AF215 present distinct textural and petrological characteristics (Fig. 2b; Table 2). Domain A has an equigranular texture (grain size <500 µm) composed of 30 % plagioclase, 37 % biotite and 31 % orthopyroxene with minor spinel, ilmenite and rare quartz (Fig. 3a). Domain B has also an equigranular texture composed of mm-sized crystals of biotite (44 %) and orthopyroxene (46 %), with rare plagioclase (8 %), cordierite, spinel and ilmenite (Fig. 3b). In both domains, local patches rich in plagioclase surrounded by ferromagnesian minerals can be interpreted in terms of leucosome and melanosome domains. Locally, a sillimanite grain occur close to the contact between domains A and B. Hercynitic spinel occurs as inclusions in orthopyroxene,

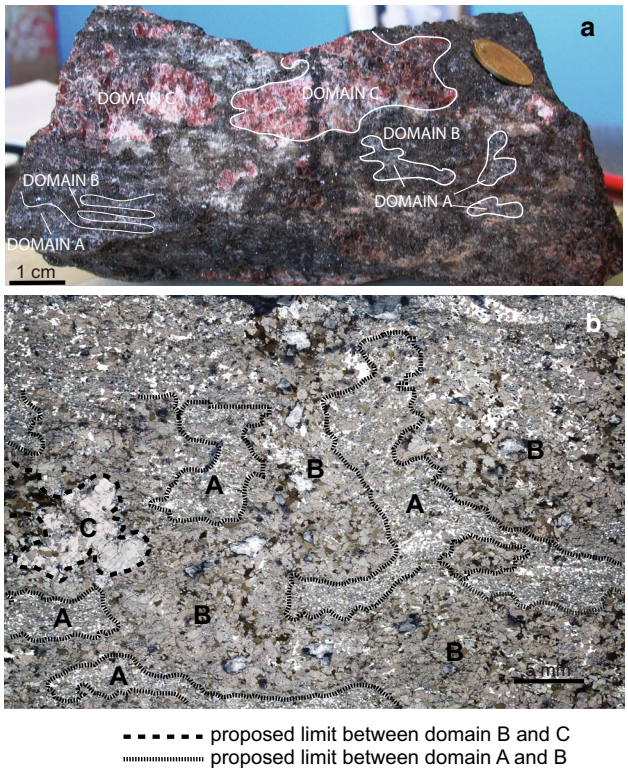

Fig. 2 **a** Picture of a hand specimen of the studied sample. Domain C is composed of garnet porphyroblasts whereas the contacts between domains A (*slightly lighter* domains) and B (*slightly darker* domains) are irregular. **b** Thin section photomicrographs showing the three domains and their borders

cordierite or plagioclase in both domains. Locally in domain B, cordierite forms rims around biotite or orthopyroxene in plagioclase-rich patches (Fig. 3b). Domain C shows inclusions (<500 μm) of orthopyroxene and biotite in cm-sized porphyroblastic garnets. Subhedral smaller garnet grains associated with ilmenite occur around garnet porphyroblasts (Fig. 3c). Garnet-spinel intergrowths occur locally. In addition, anhedral cordierite crystals (<200 μm) appear as rims between garnet and orthopyroxene belonging to domain B. The contacts between these three domains are well defined. The proportion of each domain present in the sample has been estimated by optical image analysis using the ImageJ software. Domain B dominates (~67 vol% of the rock) whereas domain A makes ~28 vol% of the rock and domain C remains minor (~5 vol% of the rock).

Mineral and domain bulk chemistry

Garnet is almandine-rich (X_{Alm} = 0.53–0.55) with the smaller garnet crystals being richer in iron (X_{Alm} = 0.61) than the porphyroblasts (Table 3). In both domains A and B, orthopyroxene shows a similar range of composition (X_{Mg} = 0.62–0.65; Al(M1) = 0.13–0.24). Except for high Al(M1) amount in orthopyroxene rims close to sillimanite crystals and higher X_{Mg} values for orthopyroxene inclusions in garnet, we could not recognise any systematics in the amount of Al(M1) according to textural position (Fig. 4). A suite of analyses of orthopyroxene inclusions in the garnet porphyroblasts of domain C show a systematic decrease in X_{Mg} and increase in Al(M1) from core to rim. Chemical zoning in garnet, orthopyroxene and biotite was not observed in any of the different domains. Cordierite rims have homogeneous magnesium-rich composition (X_{Mg} = 0.84–0.86) regardless of their textural position. Biotite displays no significant variations in X_{Mg} values according to its textural position (X_{Mg} = 0.67–0.71; see also Table 3). The content of F in biotite is negligible (up to 0.19 %). Plagioclase has high anorthite contents (An57–77) in domain A but is significantly poorer in calcium in domain B (An45–61).

Table 2 Petrographic characteristics of the three domains

	Domain A	Domain B	Domain C
Texture	Equigranular leuco/melano	Granoblastic leuco/melano	Porphyroblastic
Grain size	<500 μm	500 μm–1 mm	1 mm to cm
Contacts	To C: none	To C: well defined	To A: none
	To B: well defined	To A: well defined	To B: well defined
Assemblages	Major: Opx, Bt, Pl	Major: Opx, Bt	Major: Grt
	Minor: Spl, Sil, Ilm, Qtz	Minor: Crd, Pl, Spl, Ilm	minor: Bt, Opx as inclusions
Relevant local assemblages	Sil close to contact to B	Crd rims	Crd rims
	Spl	Spl	
Mineral abundance (in %)	Bt 37, Opx 31, Pl 30, Spl 1, Ilm 1, Qtz < 1	Bt 44, Opx 46, Pl 8, Crd 1, Ilm 1	Grt 80, Bt 19, Crd 1
Inferred chemical variations	Si/Al−	Si/Al+	
	Ca/Al+	Ca/Al−	
Total volume of rock (%)	~28	~67	~5

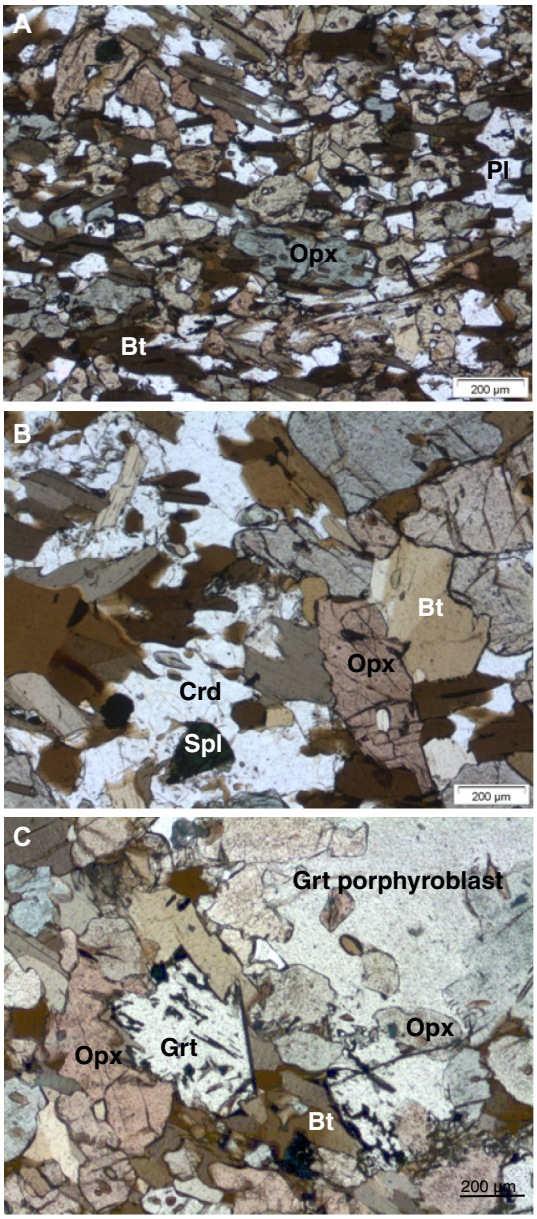

Fig. 3 Photomicrographs in plane-polarised light showing characteristic textures of the three domains. **a** Typical equigranular texture of domain A with orthopyroxene, biotite, plagioclase as well as local sillimanite and spinel. **b** Local cordierite and spinel occurrence in a leucocratic zone of domain B. **c** New garnet growth near a garnet porphyroblast rich in orthopyroxene inclusions (domain C). Abbreviations after Whitney and Evans (2010)

Concerning bulk composition, domains A and B have similar SiO_2, K_2O, Na_2O and TiO_2 contents (Table 4). Domain A is richer in Al_2O_3 and CaO than domain B, as it contains more plagioclase (Table 2). Domain B is richer in FeO and MgO as it contains more ferromagnesian phases (15.4 and 16.4 % for B; 11.8 and 12.2 % for A, respectively). The bulk composition for domain C is considered to be of similar composition as the garnet. Domains A and B show water contents of 1.7 and 2.3 wt%, respectively. This difference reflects the higher modal abundance of biotite in domain B (44 vs. 37 vol% in domain A; see Table 2). These chemical components are important to consider in the choice of the chemical system used to model the petrological evolution of these domains.

P–T conditions

Equilibrium assemblage diagrams

Figure 5a is an equilibrium assemblage diagram presenting possible paragenesis for the bulk composition of microdomain A. The observed assemblage feldspar–ilmenite–orthopyroxene–biotite–spinel–melt is stable over a large *P–T* range (850–950 °C and 0.4–0.8 GPa). Using isopleths composition of aluminium in orthopyroxene (long dashed lines) and X_{Mg} of orthopyroxene (=Mg/(Mg + Fe; short dashed lines), the peak stability field of the observed assemblage can be reduced to 830–870 °C and 0.5–0.7 GPa (represented by the grey triangle on Fig. 5a). At 0.6 GPa and 850 °C, the phase equilibrium model reasonably predicts modal abundances of 33 % plagioclase, 26 % orthopyroxene, 35 % biotite, 2 % spinel, 1 % ilmenite and no garnet, whereas the three first phases are present in equal amounts in thin section.

Geothermobarometry

Several studies investigated the "Al-in-orthopyroxene" geothermobarometer in different systems (Harley and Green 1982; Harley 1984b; Aranovich and Berman 1997; Hollis and Harley 2003; Kelsey et al. 2005). For orthopyroxene compositions coexisting with garnet (domain C; Table 3), the calibration of Harley and Green (1982) shows pressure-independent isopleths indicating equilibration temperatures between 940 and 970 °C (Fig. 5b). The calibration of Aranovich and Berman (1997) presents isopleths with a slight positive slope indicating similar temperatures between 0.7 and 0.8 GPa.

Fe–Mg exchange between garnet and orthopyroxene in direct contact indicates temperatures between 850° (Harley 1984a, b) and 960 °C (Sen and Bhattacharya 1984) at 0.9 GPa depending on the calibration of the geothermometer. Topological studies (Cenki et al. 2002; Braun et al. 2007) based on experimental work (Carrington and Harley 1995) indicate that a minimum temperature for spinel and orthopyroxene coexisting with melt is 940 °C at 0.8 GPa for a metapelitic composition. In the quartz–corundum-free grid, the appearance of spinel, orthopyroxene and melt occurs at similar temperature and pressure as mentioned before (Kelsey et al. 2005).

Table 3 Representative EMPA mineral analysis

Orthopyroxene					Garnet			Cordierite		Biotite			Plagioclase		
	Domain A	Domain A Rim to sill	Domain B	Domain C Inclusion		Domain C Porphyroblast	Domain C Smaller grain		Domain B		Domain A	Domain B		Domain A	Domain B
SiO_2	47.07	45.37	48.87	49.99	SiO_2	39.39	39.07	SiO_2	49.77	SiO_2	37.23	37.38	SiO_2	50.87	55.47
Al_2O_3	9.16	10.70	8.24	7.33	Al_2O_3	22.89	22.69	Al_2O_3	34.86	Al_2O_3	16.96	17.90	Al_2O_3	31.54	29.03
TiO_2	0.11	1.08	0.06	0.07	TiO_2	0.16	0.03	TiO_2	0.01	TiO_2	4.03	3.74	TiO_2	0.02	0.01
FeO	21.47	18.78	20.80	19.65	FeO	25.83	27.75	FeO	3.48	FeO	12.99	12.54	FeO	0.09	0.05
MgO	21.03	19.62	21.01	22.84	MgO	10.02	8.18	MgO	11.47	MgO	15.18	14.52	MgO	0.00	0.00
MnO	0.28	0.25	0.43	0.16	MnO	0.84	1.34	MnO	0.07	MnO	0.01	0.01	MnO	0.07	0.02
CaO	0.07	0.04	0.05	0.07	CaO	1.83	1.37	CaO	0.01	CaO	0.01	0.03	CaO	13.80	10.47
Na_2O	0.00	0.17	0.00	0.00	Na_2O	0.00	0.00	Na_2O	0.10	Na_2O	0.29	0.30	Na_2O	3.76	5.57
K_2O	0.02	2.57	0.00	0.00	K_2O	0.00	0.01	K_2O	0.00	K_2O	9.71	9.39	K_2O	0.04	0.06
Total	99.21	98.58	99.47	100.11	Total	100.96	100.44	Total	99.78	F	0.09	0.08	Total	100.18	100.69
										Total	96.50	95.89			
Cations (normalised to 6 oxygens)					Cations (normalised to 12 oxygens)			Cations (normalised to 18 oxygens)		Cations (normalised to 22 oxygens)			Cations (normalised to 8 oxygens)		
Si	1.76	1.72	1.82	1.83	Si	2.98	3.00	Si	4.94	Si	5.44	5.46	Si	2.31	2.48
Al	0.40	0.48	0.36	0.32	Al	2.04	2.05	Al	4.08	Al	2.92	3.08	Al	1.69	1.53
Ti	0.00	0.03	0.00	0.00	Ti	0.01	0.00	Ti	0.00	Ti	0.44	0.41	Ti	0.00	0.00
Fe	0.67	0.60	0.65	0.60	Fe	1.63	1.78	Fe	0.29	Fe	1.59	1.53	Fe	0.00	0.00
Mg	1.17	1.11	1.16	1.25	Mg	1.13	0.94	Mg	1.70	Mg	3.31	3.16	Mg	0.00	0.00
Mn	0.01	0.01	0.01	0.00	Mn	0.05	0.09	Mn	0.01	Mn	0.00	0.00	Mn	0.00	0.00
Ca	0.00	0.00	0.00	0.00	Ca	0.15	0.11	Ca	0.00	Ca	0.00	0.00	Ca	0.67	0.50
Na	0.00	0.01	0.00	0.00	Na	0.00	0.00	Na	0.02	Na	0.08	0.09	Na	0.33	0.48
K	0.00	0.12	0.00	0.00	K	0.00	0.00	K	0.00	K	1.81	1.75	K	0.00	0.00
										F	0.04	0.04			
Al(M1)	0.17	0.23	0.18	0.15	X_{Prp}	0.38	0.32	X_{Mg}	0.85	OH	3.96	3.96	% An	67	51
X_{Mg}	0.63	0.65	0.64	0.67	X_{Alm}	0.55	0.61			X_{Mg}	0.68	0.68	% Ab	33	49
					X_{Grs}	0.05	0.04								
					X_{Sps}	0.02	0.03								

X_{Mg} = Mg/(Mg + Fe) for orthopyroxene, cordierite and biotite

For garnet, X_{Prp} is Mg/(Mg + Fe + Ca + Mn), X_{Alm} is Fe/(Mg + Fe + Ca + Mn), X_{Grs} is Ca/(Mg + Fe + Ca + Mn), X_{Sps} is Mn/(Mg + Fe + Ca + Mn)

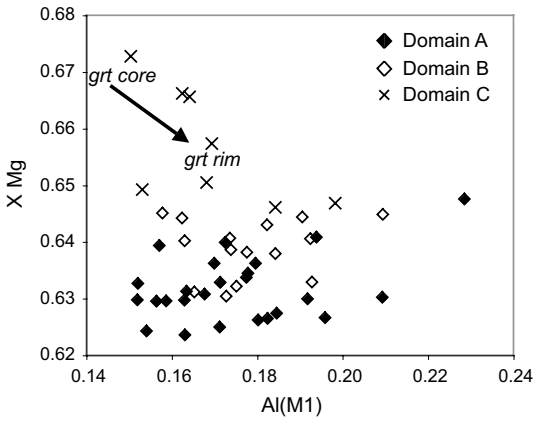

Fig. 4 Electron microprobe data of orthopyroxene composition in the three domains presented as X_{Mg} versus Al content

Table 4 Estimated bulk composition of the three domains (see text for explanations)

Bulk (wt%)	Domain A[a]	Domain B[a]	Domain C[b]
SiO_2	43.58	43.62	38.88
Al_2O_3	19.53	14.16	21.96
TiO_2	1.93	2.06	0.76
FeO	11.81	15.38	22.96
MgO	12.16	16.36	10.67
MnO	0.13	0.21	0.99
CaO	4.12	0.87	1.21
Na_2O	1.23	1.84	0.07
K_2O	3.57	4.25	1.88
H_2O	1.70	2.33	0.02
Total	99.76	101.10	99.39
Al/Si	0.53	0.38	0.69

[a] Representative mineral analysis combined with mineral abundance determined with BSE image analysis with ImageJ

[b] Garnet core composition from microprobe analysis only

The results of equilibrium assemblage modelling and geothermobarometry point to minimum peak metamorphic conditions at ca. 850 °C and 0.60 GPa for the equilibration of the sample AF215.

Thermodynamic modelling of melt loss and formation of microdomains

One of the most critical question concerning migmatitic or restitic rocks deals with the presence of melt (e.g. White and Powell 2010; Kelsey and Hand 2014): How much melt was formed and at which point? Did melt escape? To what extent had these processes an influence on the equilibrium composition of the solid phases? We have explored possible scenarios of formation for the studied sample with the help of thermodynamic modelling featuring compositional variations following the approach of White et al. (2001).

The observed mineral assemblages is restitic (Table 2), and evidence of crystallized melt is rare; therefore, we assume that melt loss occurred at some stage of the rock evolution. *T*–*X* diagrams are best suitable to model open system processes involving melt. Protolith composition shall be a mixture between the residue and melt end-members (White et al. 2001). Figure 6a is a *T*–*X* equilibrium assemblage diagram calculated in order to represent changes in assemblages for mixture compositions ranging between a restitic composition (domain A) and a typical haplogranitic melt (Table 2 in White et al. 2001). For X_{melt} ranging between 0.35 and 0.45, assemblages above the solidus (ca. 730 °C) are dominated by garnet, cordierite. These are typical incongruent phases associated to dehydration melting of biotite in metapelites (Spear et al. 1999; Johnson et al. 2001). Upon cooling (vertical path on Fig. 6a), minerals specific to metapelites occur like sillimanite (at ca. 650 °C). Our observations and models are compatible with the idea that the protolith of our sample is a metapelite, which underwent partial melting and subsequent melt loss (at melt mode of ca. 0.40 and temperatures close to the solidus; Fig. 6a).

Figure 6b is a *T*–*X* equilibrium assemblage diagram calculated in order to represent changes in assemblages for mixture compositions ranging between a restitic composition (domain B) and a typical haplogranitic melt (same approach as in Fig. 6a). Above 800 °C and for X_{melt} ranging between 0.10 and 0.25, the assemblage consisting of feldspar, biotite, orthopyroxene and melt is stable (grey field on Fig. 6b). This corresponds to the assemblage corresponding to domain A. Therefore, we suggest that domain B forms after re-melting of domain A at temperatures above 800 °C and subsequent melt loss (at melt mode of ca. 0.20). In addition, melt mode isopleths show that the new mixed rock can produce 15–30 % melt in the stability field of the mineral assemblage characteristic of domain A at HT conditions.

Discussion

Developing and preserving biotite-rich microdomains in HT rocks

In this study, we report the presence of microdomains which are composed of up to 45 % biotite and orthopyroxene associated locally to plagioclase, minor cordierite and spinel. Except for localised cordierite rims around ferromagnesian phases associated with plagioclase-rich pockets, there is no evidence for reaction textures. Each domain shows well-equilibrated granoblastic textures indicating

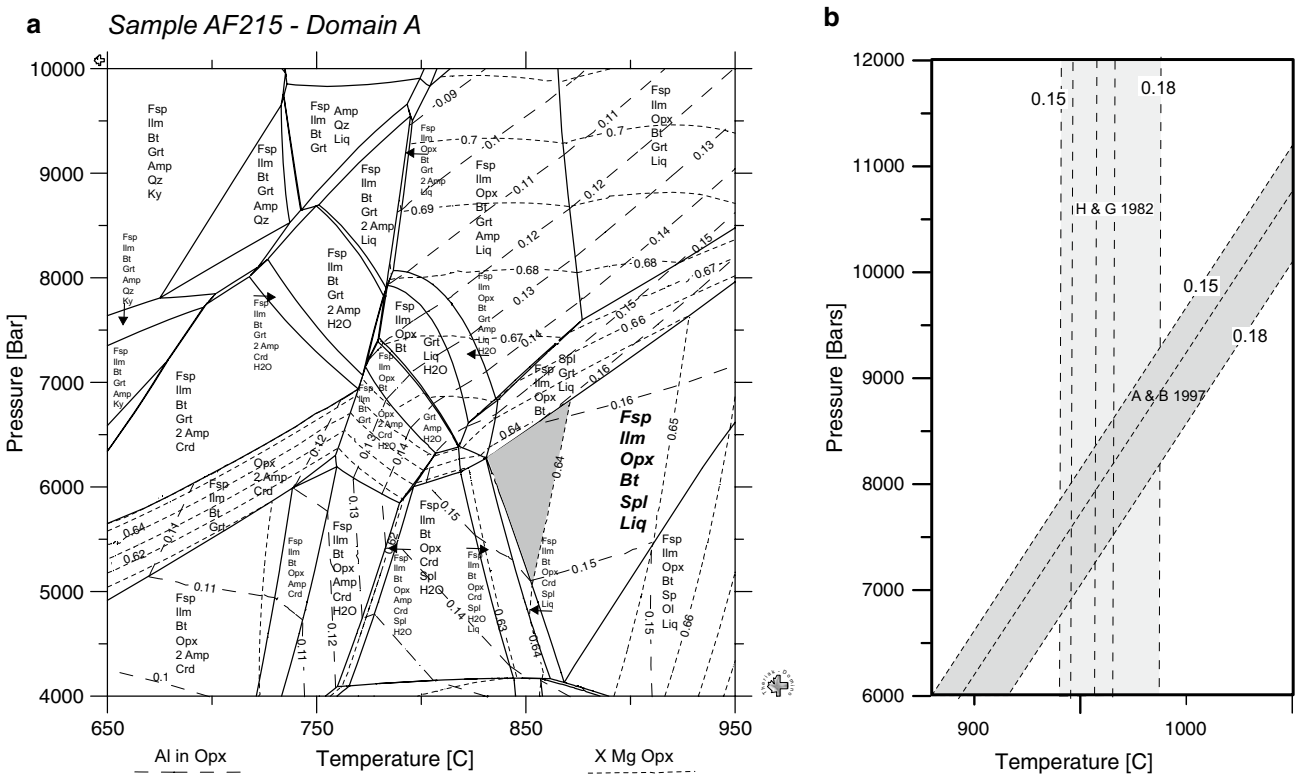

Fig. 5 **a** Modelled phase diagram using the chemical composition of domain A using Domino/Theriak (de Capitani and Petrakakis 2010) which reproduces the observed assemblage of feldspar–ilmenite–orthopyroxene–biotite–spinel–melt (in *bold italics*). Isopleths presented are related to the Al content (*long dashed lines*) and X_{Mg} [Mg/(Mg + Fe); *short dashed lines*] of orthopyroxene. Abbreviations after Whitney and Evans (2010). **b** Results from classical thermobarometry (experimentally calibrated reactions lines for aluminium contents of orthopyroxene between 0.15 and 0.18 corresponding to the measured values in the studied sample presented in Fig. 4; H & G, 1982 refers to the calibration of Harley and Green 1982; A & B 1997 refers to the calibration of Aranovich and Berman 1997)

textural equilibrium between mineral phases. Forward modelling using the bulk composition of highly restitic rocks is performed, but noting that equilibrium compositions may change drastically as a consequence of open system processes involving melt loss. Nevertheless, equilibrium *P–T* modelling for the rock (domain A) is in good agreement with classical thermobarometry (Al in Opx, Fe–Mg exchange) and point to minimum peak metamorphism at ca. 850 °C and 0.60 GPa. Based on *T–X* models involving the composition of the observed domains, we suggest that these heterogeneities result from at least two melting events accompanied by melt loss. In addition, the effect of subsolidus water loss on melt fertility of crustal rocks has recently been explored (Webb et al. 2015) and may be involved at least in parts to explain the genesis of the studied rocks.

Our modelling suggests that sample protolith is a metapelite that experienced melt loss which operated as a bulk compositional modifier. Nevertheless the nature of the protolith and the degree of inheritance of primary chemical heterogeneities due to compositional banding may be considered. Diener et al. (2008) showed that orthopyroxene-rich quartz-saturated granulites from the Strangways Range in Australia derive from cordierite–orthoamphibole gneisses and that compositional changes associated to melt loss from a pelitic protolith are not sufficient to account for the unusual compositions. The compositions reported by Diener et al. (2008) are attributed to metamorphosed metasomatic volcanic rocks. However, composition of microdomains from the rock studied here are significantly richer in alkalis (Na, K), amphibole is absent, cordierite is insignificant, and biotite is widespread due to the extraction of melt (which left residual biotite in the source), In this study, we have shown that a mixture of a restitic composition corresponding to domain A together with a melt generates typical pelitic assemblages (Fig. 6a). Recently, Ganne et al. (2014) described metapelitic kinzigite (VG49) in the same area of the Antananarivo Block. These are composed of plagioclase, quartz, biotite, cordierite, garnet and sillimanite. These authors infer *P–T* conditions of equilibration of their metapelitic sample during the early D1 tectonic phase (Martelat et al. 1999) that corresponds to the conditions calculated in this study (pressure at ca. 0.6 GPa and temperature >850 °C). This chemical,

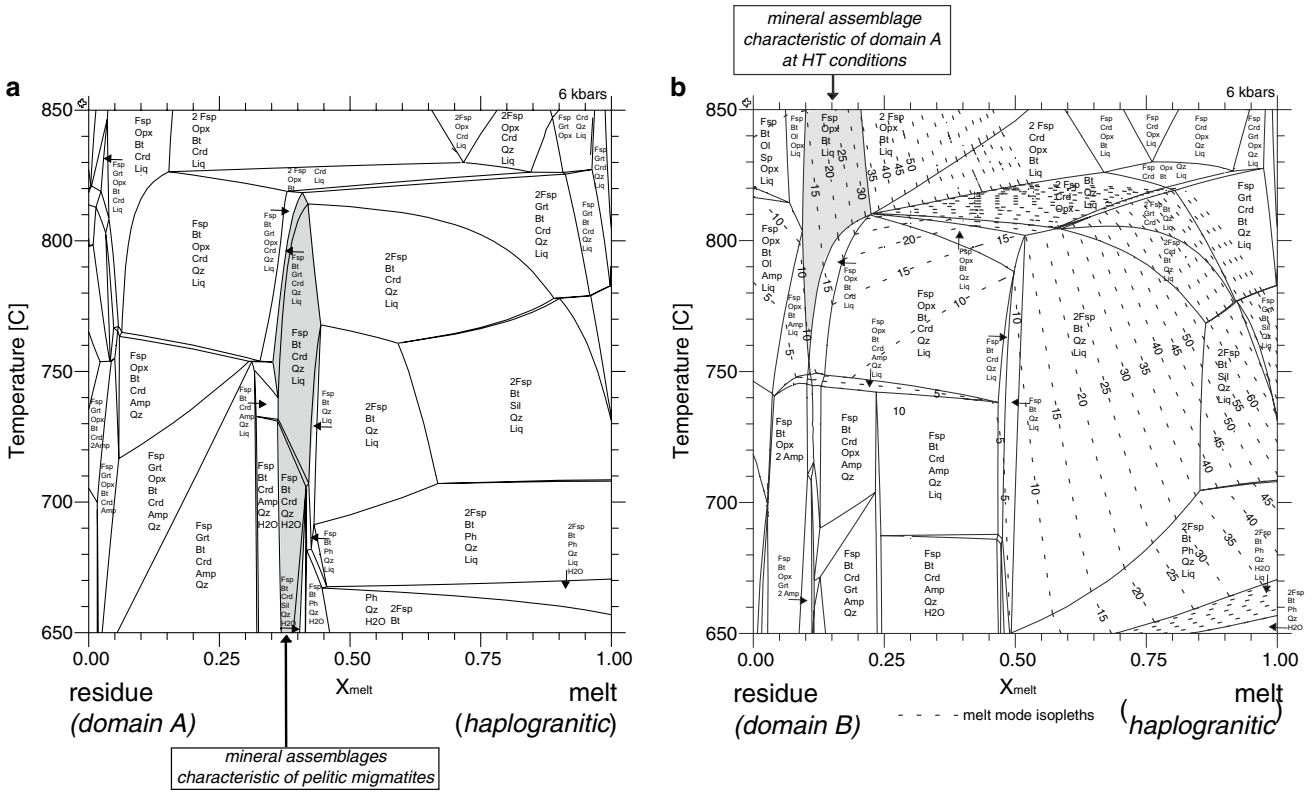

Fig. 6 Binary *T–X* models calculated at 6 kbar between a restitic composition [domain A in (**a**) and domain B in (**b**)] and a typical haplogranitic melt (from White et al. 2001) using Domino/Theriak (de Capitani and Petrakakis 2010). Abbreviations after Whitney and Evans (2010). *Dashed lines* in (**b**) represent melt mode isopleths

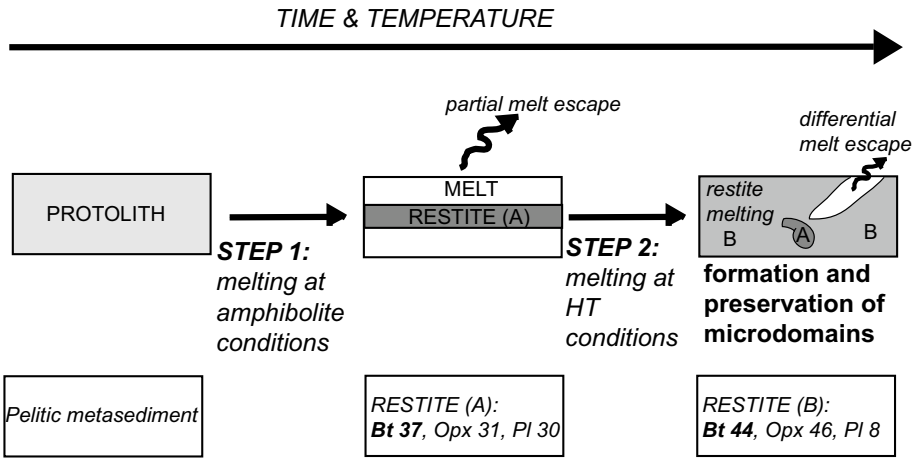

Fig. 7 Sketch depicting the formation and evolution of microdomains in the studied sample

petrological and geological evidence argue in favour of a pelitic protolith for the studied sample.

The inferred evolution of this sample with time and temperature is shown on Fig. 7. In the first step, a homogeneous metapelitic protolith (see above) melts at amphibolite facies conditions yielding a restite (preserved in domain A) and a melt that is extracted. In the second step, this restite re-melts at higher temperature resulting in the formation of domain B followed by renewed melt escape. We suggest that the observed microdomains are formed and preserved due to sequential melt escape. Unfortunately, evidence for melt is scarce (local plagioclase-rich patches), but our thermodynamic modelling attests for the presence of melt (produced and escaped) at different stages of microdomains formation. If melt would have resided within the rock, melt-consuming reactions (Cenki et al. 2002) is expected

to occur and their products to from (Kriegsman 2001; e.g. coronas of ferromagnesians phases around incongruent phases). These textures are not observed in the studied sample. Generally, the preservation of granulite facies mineral assemblages is often linked to melt loss processes (e.g. Brown 2010). In addition, other authors has proposed a similar scenario of at least two partial melting events as pre-conditioning (that prevents buffering of temperature through pervasive partial melts) of the crust and appear to be a prerequisite in order to reach UHT conditions (Vielzeuf et al. 1990).

The formation of H_2O-rich biotite in residual rocks and water in the deep crust

In this study, we describe HT granulite which contains a large amount of biotite (up to 45 % of the rock) stable with orthopyroxene. At HT granulite facies rocks, biotite is expected to be F-rich (Bose et al. 2005) and not so OH-rich, with an enrichment in F as temperature increases, while biotite is progressively replaced by anhydrous minerals or melt (e.g. Mouri et al. 1996; Motoyoshi and Hensen 2001; Adjerid et al. 2008). It has been shown that F-rich biotite occurs in nature with UHT minerals (e.g. osumilite), whereas thermodynamic modelling indicates that this should not occur with normal OH-rich biotite (this study). Various explanations for this should be considered. Firstly, this low fluorine content might be a primary feature of the bulk rock and fluid composition. Mouri et al. (1996) proposed that metamorphosed hydrothermally altered mafic rocks are good candidates to show F-enrichment. As we propose that the protolith is a classic pelite, it is well possible that the bulk is fluorine poor. Secondly, by removing granitic melts from the pelitic sample, the rock might run out of reactant before running out of hydrous, prograde biotite. Similarly, Nahodilova et al. (2011) showed that the preservation of prograde minerals (garnet in their case) is bounded to complete melt loss. Thirdly, Motoyoshi and Hensen (2001) have suggested that melt-consuming reactions involving a F-rich fluid lead to the formation of F-rich biotite. However, we have suggested that melt probably escaped as formed and did not reside significantly in the source. Fourthly, experiments conducted under water-saturated conditions (Gardien et al. 1995), indicated that hydrous biotite can be stable up to 950 °C (at 1 GPa). This possibility shall be further explored for the genesis of the studied sampled. Finally, White and Powell (2010) have shown that diffusion of water from the leucosome to the residue may occur upon cooling when biotite crystallises in the residue that leads to an increase of the chemical potential of water in the melt. In that case, chemical gradients favour the crystallisation of anhydrous minerals in the melt and hydrous minerals in the residue. The common observation that several granulites have no (or only tiny bit) of hydrous phases (Clarke et al. 2005; Clemens 2006) raises the question of the origins of a dry lower crust (Frost and Bucher 1994; Yardley and Valley 1997). Melt extraction leaves excess biotite in the source that forms highly refractory domains where water can be preserved in the granulite facies in the deep crust.

Extrapolation at crustal scale

Although our study focusses on dm-scale samples, the inferred processes may be relevant at the scale of the entire lower crust. Classically, the lower crust is viewed as an anhydrous granulite-facies domain, produced by the progressive loss of water during HT metamorphism and in situ melting (Powell 1983; Thompson 1990). Our study proposes an alternative view, in which the continuous extraction of the produced melt may leave excess, residual domains enriched in H_2O-rich biotite in the source. These two processes (anhydrous granulitisation and biotite enrichment) may act coevally and lead to the formation of a strongly heterogeneous lower crust. These mineralogical heterogeneities imply strong rheological contrasts with the coexistence of biotite poor (anhydrous granulite) and biotite-rich domains in the deep crust. Biotite is a weak mineral (Kronenberg et al. 1990), compared with common lower crust minerals (plagioclase, pyroxene, Bürgmann and Dresen 2008). Furthermore, in polymineralic assemblages, the weakest mineral may control the strength and therefore strongly weakens the entire assemblage (Handy et al. 1999; Gueydan et al. 2014). We may therefore propose a strongly heterogeneous ductile lower crust, at least locally, in which the coexistence of creep and shear failure is possible.

Conclusions

The observation of these HT rocks from Madagascar can be summarised as follows: (a) a large amount of biotite and orthopyroxene can be stable at granulite facies conditions; (b) microdomains are formed and preserved in meta-sedimentary protolith associated to melt generation and melt loss; (c) the presence of H_2O-rich biotite and heterogeneities in the middle/lower crust in which excess biotite can occur in source regions after melt escape. These processes imply that water can be preserved in highly refractory domains of the deep crust. These conditions might not be valid for the entire lower crust but may be important locally and have rheological consequences.

Acknowledgments We thank A. Fernandez and G. Schreurs for providing the samples. Financial support from Swiss National Fund is greatly acknowledged for our work in Madagascar (Grant Nos.

2000-65306.01, 200020-105453/1 and 200020-109320) and for the use of the electron microprobe at the University of Bern (Grant 200021-103479/1). We thank Ch. De Capitani for updating the database used by the DOMINO/THERIAK software. G. Schreurs, P. Pitra, I. Braun and two anonymous reviewers are thanked for their highly constructive comments on earlier versions of the manuscript. V. Pease is thanked for editorial handling.

References

Adjerid Z, Ouzegane K, Godar G, Kienast JR (2008) First report of ultrahigh-temperature sapphirine + spinel + quartz and orthopyroxene + spinel + quartz parageneses, discovered in Al–Mg granulite from Khanfous area (In Ouzzal metacraton, Hoggar, Algeria). Geological Society, London, Special Publications, vol 297, pp 147–167

Aranovich LY, Berman RG (1997) A new orthopyroxene–garnet thermometer based on reversed Al_2O_3 solubility in FeO–Al_2O_3–SiO_2 orthopyroxene. Am Mineral 82:345–353

Archibald DB, Collins AS, Foden JD, Payne JL, Taylor R, Holden P, Razakamanana T, Clark C (2015) Towards unravelling the Mozambique Ocean conundrum using a triumvirate of zircon isotopic proxies on the Ambatolampy Group, central Madagascar. Tectonophysics **(in press)**

Baldwin JA, Powell R, Brown M, Moraes R, Fuck RA (2005) Modelling of mineral equilibria in ultrahigh-temperature metamorphic rocks from the Anapolis-Itaucu Complex, central Brazil. J Metamorph Geol 23:511–531

Berger A, Gnos E, Schreurs G, Fernandez A, Rakotondrazafy M (2006) Late Neoproterozoic, Ordovician and Carboniferous events recorded in monazites from southern-central Madagascar. Precambr Res 144:278–296

Bose S, Das K, Fukuoka M (2005) Fluorine content of biotite in granulite-grade metapelitic assemblages and its implications for the Eastern Ghats granulites. Eur J Mineral 17:665–674

Braun I, Cenki-Tok B, Paquette JL, Tiepolo M (2007) Petrology and geochronology of sapphirine–quartz-bearing metapelites from Rajapalayam, Madurai Block, southern India: evidence for polyphase Neoproterozoic high-grade metamorphism. Chemical Geology 241:129–147

Brouwer FM, Engi M (2005) Staurolite and other high-Alumina phase in Alpine eclogite: analysis of domain evolution. Can Mineral 43:105–128

Brown M (2002) Retrograde processes in migmatites and granulites revisited. J Metamorph Geol 20(1):25–40

Brown M (2010) Melting of the continental crust during orogenesis: the thermal, rheological, and compositional consequences of melt transport from lower to upper continental crust. Can J Earth Sci 47:655–694

Buddington AF (1952) Chemical petrology of some metamorphosed Adirondack gabbroic, syenitic and quartz-syenitic rocks. Am J Sci Bowen 37:84

Bürgmann R, Dresen G (2008) Rheology of the lower crust and upper mantle: evidence from rock mechanics, geodesy, and field observations. Annu Rev Earth Planet Sci 36(1):531–567

Carrington D, Harley SL (1995) Partial melting and phase-relations in high-grade metapelites—an experimental petrigenetic grid in the KFMASH system. Contrib Miner Petrol 120(3–4):270–291

Cenki B, Kriegsman LM, Braun I (2002) Melt-producing and melt-consuming reactions in the Achankovil cordierite gneisses, South India. J Metamorph Geol 20(6):543–561

Clarke GL, Daczko NR, Klepeis KA, Rushmer T (2005) Roles for fluid and/or melt advection in forming high-P mafic migmatites, Fiordland, New Zealand. J Metamorph Geol 23:557–567

Clemens JD (2006) Melting of the continental crust: fluid regimes, melting reactions, and source-rock fertility. In: Brown M, Rushmer T (eds) Evolution and differentiation of the continental crust. Cambridge University Press, Cambridge, pp 297–331

Collins AS (2006) Madagascar and the amalgamation of Central Gondwana. Gondwana Res 9:3–16

Cox R, Coleman DS, Chokel CB, DeOreo SB, Collins AS, Kröner A, DeWaele B (2004) Proterozoic tectonostratigraphy and paleogeography of central Madagascar derived from detrital zircon U–Pb age populations. J Geol 112:379–400

de Capitani C, Brown TH (1987) The computation of chemical equilibrium in complex systems containing non-ideal solutions. Geochim Cosmochim Acta 51:2639–2652

de Capitani C, Petrakakis K (2010) The computation of equilibrium assemblage diagrams with Theriak/Domino software. Am Mineral 95:1006–1016

Diener JFA, Powell R, White RW, Holland TJB (2007) A new thermodynamic model for clino- and orthoamphiboles in the system Na_2O–CaO–FeO–MgO–Al_2O_3–SiO_2–H_2O–O. J Metamorph Geol 25:631–656

Diener JFA, White RW, Powell R (2008) Granulite facies metamorphism and subsolidus fluidabsent reworking, Strangways Range, Arunta Block, central Australia. J Metamorph Geol 26:603–622

Frost BR, Bucher K (1994) Is water responsible for geophysical anomalies in the deep continental crust—a petrological perspective. Tectonophysics 231(4):293–309

Ganne J, Nédélec A, Grégoire V, Gouy S, de Parseval P (2014) Tracking Late-Pan-African fluid composition evolution in the ductile crust of Madagascar: insight from phase relation modelling of retrogressed gneisses (province of Fianarantsoa). J Afr Earth Sci 94:100–110

Gardien V, Thompson AB, Grujic D, Ulmer P (1995) Experimental melting of biotite + plagioclase + quartz ± muscovite assemblages and implications for crustal melting. J Geophys Res 100(B8):581–591

Giese J, Berger A, Schreurs G, Gnos E (2011) The timing of the tectonometamorphic evolution at the Neoproterozoic–Phanerozoic boundary in central southern Madagascar. Precambr Res 185:131–148

Goncalves P, Nicollet C, Montel JM (2004) Petrology and in situ U–Th–Pb monazite geochronology of ultrahigh-temperature metamorphism from the Andriamena mafic unit, north-central Madagascar. Significance of a petrographical *P–T* path in a polymetamorphic context. J Petrol 45(10):1923–1957

Gueydan F, Précigout J, Montési LGJ (2014) Strain weakening enables continental plate tectonics. Tectonophysics 631:189–196. doi:10.1016/j.tecto.2014.02.005

Handke MJ, Tucker RD, Ashwal LD (1999) Neoproterozoic continental arc magmatism in west-central Madagascar. Geology 27:351–354

Handy MR, Wissing SB, Streit LE (1999) Frictional-viscous flow in mylonite with varied bimineralic composition and its effect on lithospheric strength. Tectonophysics 303:175–191

Harley SL (1984a) An experimental study of the partitioning of the Fe and Mg between garnet and orthopyroxene. Contrib Miner Petrol 86:359–373

Harley SL (1984b) The solubility of alumina in orthopyroxene coexisting with garnet in FeO–MgO–Al_2O_3–SiO_2 and CaO–FeOMgO–Al_2O_3–SiO_2. J Petrol 25:665–696

Harley SL (1998a) On the occurrence and characterization of ultrahigh-temperature crustal metamorphism. In: Treloar PJ, O'Brien PJ (eds) What drives metamorphism and metamorphic reactions? vol 138. Geological Society Special Publications, London, pp 81–107

Harley SL (1998b) Ultrahigh temperature granulite metamorphism (1050 °C, 12 kbar) and decompression in garnet

(Mg70)–orthopyroxene–sillimanite gneisses from the Rauer Group, East Antarctica. J Metamorph Geol 16(4):541–562
Harley SL (2008) Refining the *P–T* records of UHT crustal metamorphism. J Metamorph Geol 26(2):125–154
Harley SL, Green DH (1982) Garnet–orthopyroxene barometry for granulites and peridotites. Nature 300:697–701
Harley SL, Hensen BJ, Sheraton JW (1990) Two-stage decompression in orthopyroxene–sillimanite granulites from Forefinger Point, Enderby Land, Antarctica: implication for the evolution of the Archaean Napier Complex. J Metamorph Geol 8:591–613
Holland TJB, Powell R (1998) An internally consistent thermodynamic dataset for phases of petrological interest. J Metamorph Geol 16:243–309
Hollis JA, Harley SL (2003) Alumina solubility in orthopyroxene coexisting with sapphirine and quartz. Contrib Miner Petrol 144(4):473–483
Jackson J (2002) Strength of the continental lithosphere: time to abandon the jelly sandwich? GSA Today 12(9):4–10
Johnson T, Hudson N, Droop G (2001) Partial melting in the Inzie Head gneisses: the role of water and a petrogenetic grid in KFMASH applicable to anatectic pelitic migmatites. J Metamorph Geol 19:99–118
Jöns N, Schenk V, Appel P, Razakamanana T (2006) Two-stage metamorphic evolution of the Bemarivo Belt of northern Madagascar: constraints from reaction textures and in situ monazite dating. J Metamorph Geol 24:329–347
Kelsey DE (2008) On ultrahigh-temperature crustal metamorphism. Gondwana Res 13(1):1–29
Kelsey D, Hand M (2014) On ultrahigh temperature crustal metamorphism: phase equilibria, trace element thermometry, bulk composition, heat sources, timescales and tectonic settings. Geosci Front. doi:10.1016/j.gsf.2014.09.006
Kelsey DE, White RW, Powell R (2005) Calculated phase equilibria in K_2O–FeO–MgO–Al_2O_3–SiO_2–H_2O for silica-undersaturated sapphirine-bearing mineral assemblages. J Metamorph Geol 23:217–239
Kohn MJ, Spear FS (2001) GTB. Computer program. http://ees2.geo.rpi.edu/MetaPetaRen/GTB_Prog/GTB.html
Kriegsman LM (2001) Partial melting, partial melt extraction and partial back reaction in anatectic migmatites. Lithos 56:75–96
Kronenberg AK, Kirby SH, Pinkston J (1990) Basal slip and mechanical anisotropy of biotite. J Geophys Res 95(B12):19257–19278
Kröner A, Hegner E, Collins AS, Windley BF, Brewer TS, Razakamanana T, Pidgeon RT (2000) Age and magmatic history of the Antananarivo block, central Madagascar, as derived from zircon geochronology and Nd isotopic systematics. Am J Sci 300:251–288
Martelat JE, Lardeaux JM, Nicollet C, Rakotondrazafy R (1999) Exhumation of granulites within a transpressive regime: an example from southern Madagascar. Gondwana Res 2:363–368
Martelat JE, Lardeaux JM, Nicollet C, Rakotondrazafy R (2000) Strain pattern and late Precambrian deformation history in southern Madagascar. Precambr Res 102:1–20
McDade P, Harley SL (2001) A petrogenetic grid for aluminous granulite facies metapelites in the KFMASH system. J Metamorph Geol 19:45–59
McFarlane CRM, Carlson WD, Connelly JN (2003) Prograde, peak, and retrograde *P–T* paths from aluminium in orthopyroxene: high-temperature contact metamorphism in the aureole of the Makhavinekh Lake Pluton, Nain Plutonic Suite, Labrador. J Metamorph Geol 21(5):405–423
McKenzie D, Jackson J (2002) Conditions for flow in the continental crust. Tectonics 21(6):1055. doi:10.1029/2002TC001394
McMillan A, Harris NBW, Holness M, Ashwal L, Keley S, Rambeloson R (2003) A granite–gabbro complex from Madagascar: constraints on melting of the lower crust. Contrib Miner Petrol 145:585–599
Motoyoshi Y, Hensen BJ (2001) F-rich phlogopite stability in ultrahigh-temperature metapelites from the Napier Complex, East Antarctica. Am Mineral 86:1404–1413
Mouri H, Guiraud M, Hensen BJ (1996) Petrology of phlogopite–saphirine-bearing Al–Mg granulites from Ihouhaouhene, In Ouzzal, Hoggar, Algeria: an example of phlogopite stability at high temperature. J Metamorph Geol 14:725–738
Nahodilova R, Faryad SW, Dolejs D, Tropper P, Konzett J (2011) High-pressure partial melting and melt loss in felsic granulites in the Kutna Hora complex, Bohemian Massif (Czech Republic). Lithos 125:641–658
Powell R (1983) Fluids and melting under upper amphibolite facies conditions. J Geol Soc Lond 140:629–633
Raith JG, Harley SL (1998) Low-*P*/high-*T* metamorphism in the Okiep Copper District, western Namaqualand, South Africa. J Metamorph Geol 16:281–305
Rickers K, Raith M, Dasgupta S (2001) Multistage reaction textures in xenolithic high-MgAl granulites at Anakapalle, Eastern Ghats Belt, India: examples of contact polymetamorphism and infiltration-driven metasomatism. J Metamorph Geol 19:561–580
Sajeev K, Osanai Y (2004) Ultrahigh-temperature metamorphism (1150 °C, 12 kbar) and multistage evolution of Mg-, Al-rich granulites from the central Highland Complex, Sri Lanka. J Petrol 45(9):1821–1844
Scherrer NC, Engi M, Gnos E, Jakob V, Liechti A (2000) Monazite analysis; from sample preparation to microprobe age dating and REE quantification. Schweiz Mineral Petrogr Mitt 80:93–105
Sen SK, Bhattacharya A (1984) An orthopyroxene-garnet thermometer and its application to the Madras charnockites. Contrib Miner Petrol 88:64–71
Spear FS, Kohn MJ, Cheney JT (1999) *P–T* paths from anatectic pelites. Contrib Miner Petrol 134:17–32
Thompson AB (1990) Heat, fluids, and melting in the granulite facies. In granulites and crustal evolution. In: Vielzeuf D, Vidal P (eds) NATO ASi series. Series C: mathematical and physical sciences, vol 311. D. Reidel, Dordrecht, pp 37–57
Tòth TM, Grandjean V, Engi M (2000) Polyphase evolution and reaction sequence of compositional domains in metabasalt: a model based on local chemical equilibrium and metamorphic differentiation. Geol J 35:163–183
Tucker RD, Ashwal LD, Handke MJ, Hamilton MA, LeGrange M, Rambeloson RA (1999) U–Pb geochronology and isotope geochemistry of the Archean and Proterozoic rocks of north-central Madagascar. J Geol Soc Lond 107:135–153
Tucker RD, Kusky TM, Buchwaldt R, Handke MJ (2007) Neoproterozoic nappes and superposed folding of the Itremo Group. Gondwana Res 12:356–379
Tucker RD, Roigb JY, Moinec B, Delorb C, Peters SG (2014) A geological synthesis of the Precambrian shield in Madagascar. J Afr Earth Sci 94:9–30
Turner FJ (1981) Metamorphic petrology, mineralogical and field aspects, 2nd edn. McGraw-Hill, New York
Vielzeuf D, Clemens JD, Pin C, Minet E (1990) Granites, granulites and crustal differentiation. In: Vielzeuf D, Vidal P (eds) Granulites and Cruistal evolution. NATO Scientific Publication. Kluwer Academic Publishers, Dordrecht, pp 59–85
Webb G, Powell R, McLaren S (2015) Phase equilibria constraints on the melt fertility of crustal rocks: the effect of subsolidus water loss. J Metamorph Geol 33:147–165
White RW, Powell R (2010) Retrograde melt–residue interaction and the formation of near-anhydrous leucosomes in migmatites. J Metamorph Geol 28(6):579–597
White RW, Powell R, Holland TJB (2001) Calculation of partial melting equilibria in the system Na_2O–CaO–K_2O–FeO–MgO–Al_2O_3–SiO_2–H_2O (NCKFMASH). J Metamorph Geol 19:139–153

White RW, Powell R, Clarke GL (2002) The Interpretation of reaction textures in Fe-rich metapelitic granulites of the Musgrave Block, central Australia: Constraints from mineral equilibria calculations in the system K_2O–FeO–MgO–Al_2O_3–SiO_2–H_2O–TiO_2–Fe_2O_3. J Metamorph Geol 20:41–55

White RW, Powell R, Halpin JA (2004) Spatially-focussed melt formation in aluminous metapelites from Broken Hill, Australia. J Metamorph Geol 22:825–845

White RW, Powell R, Holland TJB (2007) Progress relating to calculation of partial melting equilibria for metapelites. J Metamorph Geol 25(5):511

Whitney DL, Evans BW (2010) Abbreviations for names of rock-forming minerals. Am Mineral 95:185–187

Windley BF, Razafiniparany A, Razakamanana T, Ackermand D (1994) Tectonic framework of the Precambrian of Madagascar and its Gondwana connections—a review and reappraisal. Geol Rundsch 83:642–659

Yardley BWD, Valley JW (1997) The petrologic case for a dry lower crust. J Geophys Res Solid Earth 102(B6):12173–12185